Bioorganic & Medicinal Chemistry Letters 23 (2013) 6269–6273

Contents lists available at ScienceDirect

Bioorganic & Medicinal Chemistry Letters

journal homepage: www.elsevier.com/locate/bmcl

Identification and profiling of 3,5-dimethyl-isoxazole-4-carboxylic acid [2-methyl-4-((2*S*,3′*S*)-2-methyl-[1,3′]bipyrrolidinyl-1′-yl)phenyl] amide as histamine H_3 receptor antagonist for the treatment of depression

Zhongli Gao [a,*], William J. Hurst [b,†], Werngard Czechtizky [d], Daniel Hall [b], Nicolas Moindrot [c], Raisa Nagorny [b], Philippe Pichat [c], David Stefany [b], James A. Hendrix [b,‡], Pascal G. George [c]

[a] LGCR SMRPD Chemical Research, Sanofi US, 153-1-122, 153 2nd Ave, Waltham, MA 02451, USA
[b] Sanofi US, Route 202-206, PO Box 6800, Bridgewater, NJ 08807, USA
[c] Sanofi R&D, 1 Avenue Pierre Brossolette, Chilly-Mazarin, France
[d] Sanofi R&D, Deutschland GmbH, Industriepark Hoechst, Frankfurt, Germany

ARTICLE INFO

Article history:
Received 20 August 2013
Revised 24 September 2013
Accepted 25 September 2013
Available online 3 October 2013

Keywords:
Histamine H_3 receptor antagonist/inverse agonist
Forced swimming test
Experimental models of anxiety and depression
Anxiety
Depression

ABSTRACT

Lead optimization guided by histamine H_3 receptor (H_3R) affinity and calculated physico-chemical properties enabled simultaneous improvement in potency and PK properties leading to the identification of a potent, selective, devoid of hERG issues, orally bioavailable, and CNS penetrable H_3R antagonist/inverse agonist **3h**. The compound was active in forced-swimming tests suggesting its potential therapeutic utility as an anti-depressive agent. This Letter further includes its cardiovascular and neuropsychological/behavioral safety assessments.

The histamine H_3 receptor (H_3R),[1] a G-protein coupled receptor, is largely expressed in the anterior part of the cortex, in the hippocampus, striatum, and to a lesser extent in the hypothalamus and spinal cord. It is a pivotal presynaptic autoreceptor and heteroreceptor modulating the synthesis and release of histamine and other neurotransmitters, including acetylcholine (ACh), dopamine (DA), and norepinephrine (NE). Cloning of H_3R uncovered the existence of isoforms, inter-species pharmacological differences and a high constitutive (spontaneous) activity of the receptor.[2–5] Many isoforms of human H_3R have been identified.[6–8] The full length 445aa configuration appears to be the most functionally dominant and abundantly expressed. In addition, at least another 19 isoforms have been reported for the human H_3R. Several additional isoforms have also been identified in rat, guinea pig, and mouse. Not surprisingly, this level of complexity of expression and isoforms of H_3R have invoked more complexity in in vivo H_3R biology and interesting therapeutic applications,[9–14] such as Alzheimer's disease,[15,16] attention deficit hyperactivity disorder,[17] schizophrenia,[18–20] sleep disorder,[21] neuropathic pain,[22] and obesity.[23] Many structurally diverse H_3R antagonists have been reported and a few have advanced into development (for review articles, see Refs. 24,25). In this Letter, we will describe our continued lead optimization effort which led to the identification of a novel, potent, selective and orally efficacious H_3R antagonist/inverse agonist as one of several pre-development candidates.

Previous work[26,27] from our group revealed a series of compounds, represented by 5-fluoro-2-methyl-*N*-[2-methyl-4-(2-methyl[1,3′]bipyrrolidinyl-1′-yl)phenyl] benzamide (**1**), that displayed oral activity in a mouse food intake inhibition model. However, the compound exhibited unacceptably high affinity towards the hERG channel (IC_{50} = 0.48 μM). Furthermore, the four stereoisomers of **1** were synthesized and evaluated[28] hoping that one specific stereoisomer retained high H_3R affinity while devoid of hERG channel inhibition. Interestingly, the *S*,*S* diastereomer (**2**)

* Corresponding author. Tel.: +1 781 434 3635.
E-mail addresses: zhongli.gao@sanofi.com (Z. Gao), william.hurst@sanofi.com (W.J. Hurst), jhendrix@oligomerix.com (J.A. Hendrix).
† Address: Sanofi US, 55C-420A, 55 Corporate Drive, Bridgewater, NJ 08807, USA. Tel.: +1 908 981 3723.
‡ Current address: Oligomerix Inc., 3960 Broadway, Suite 340D, New York, NY 10032, USA. Tel.: +1 212 568 0365.

0960-894X/$ - see front matter © 2013 Elsevier Ltd. All rights reserved.
http://dx.doi.org/10.1016/j.bmcl.2013.09.081

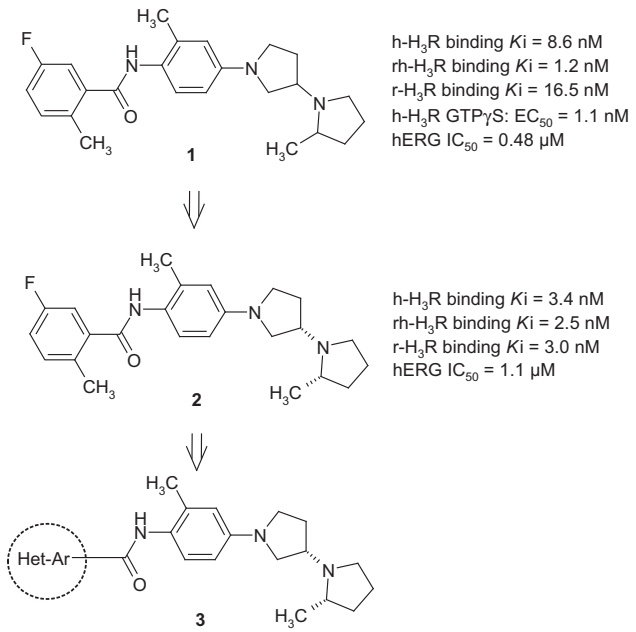

Figure 1. Lead structures of the H_3R antagonists/inverse agonists and design strategies.

showed superior in vitro H_3R affinity. However, all four stereoisomers displayed similar hERG channel affinities indicating that the elevated hERG affinity might be due to the high lipophilicity of **1** ($c\log P = 3.2$). Thus, we focused our attention towards finding a potential drug candidate with similar or better H_3R activity as **2** but an acceptable hERG profile. Besides the hERG issue, we also set up a criterion to discover an H_3R antagonist/inverse agonist with low risk of potential phospholipidosis induction, one of the common issues of H_3R ligands reported in the literature.[29,30]

To address the hERG issue, we used $c\log P$ and PSA to guide the design of new compounds. This strategy was echoed by Levoin's[31] QSAR in which he stated that the lipophilic character of the molecules (the sum of atomic polarizabilities, $c\log P$, $c\log D$), as well as aromatic tendency reflect most important aspects for hERG affinity.

Phospholipidosis is a storage disorder resulting in excessive accumulation of phospholipids in lysosomes of the tissues. The cause is not well defined. However, an amphiphilic character of molecules displays a high risk of inducing phospholipidosis. In order to increase our odds to identify H_3R ligands with low risk of phospholipidosis induction potential, we screened compounds using an in silico phospholipidosis model.[32,33] Given the fact that H_3R is a biogenic amine receptor and our current lead compound possessed a basic amine, it was hypothesized that lowering the pK_a and increasing the polarity (lowering $c\log P$ and increasing polar surface area, PSA) should be the most direct way to bring the

Table 1
rh-H_3R affinity and calculated physico-chemical properties

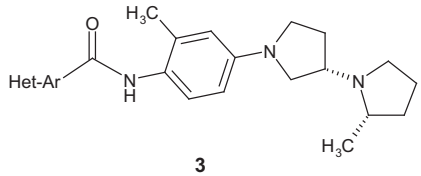

No.	Het-Ar	rh-H_3R binding[a] K_i (nM)	pK_a (basic center)	$c\log P$	$c\log D_{7.4}$	MW	PSA (Å^2)
2		2.5	10.1	3.2	0.7	395	36
3a	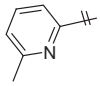	1.4	10.1	3.3	0.8	378	49
3b	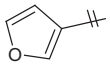	1.8	10.1	3.0	0.5	353	49
3c	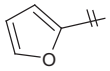	3.9	10.1	2.1	−0.4	353	49
3d	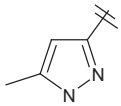	4.7	12.1	1.7	−0.8	367	64
3e	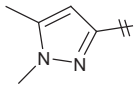	10.8	10.1	1.6	−0.8	381	53
3f	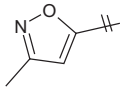	1.1	10.1	2.0	−0.5	368	62
3g	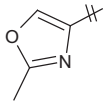	4.6	10.1	2.8	0.4	368	62
3h	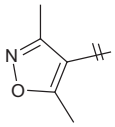	0.4	10.1	2.8	0.4	382	62

[a] Binding assay was performed as in Ref. 26; K_i data were presented as an average of multiple experiments ($n \geqslant 3$). Standard deviation <50%; ND = not determined.

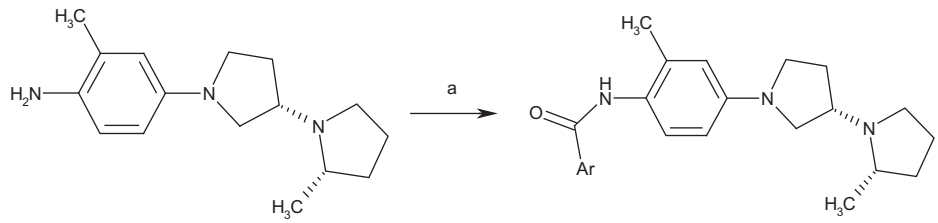

4 3

Scheme 1. Syntheses of analogs **3a**–**3h**. Reagents and conditions: (a) ArCOCl, CH_2Cl_2, pyridine, rt, 16 h, 62–80% yield.

Table 2
rh-H_3R affinity and calculated physico-chemical properties

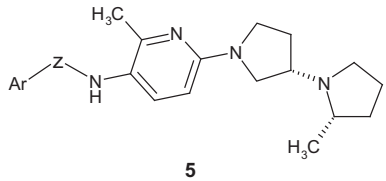

5

No.	Ar	Z	rh-H_3R binding K_i[a] (nM)	pK_a	$c\log P$	$c\log D_{7.4}$	MW	PSA (Å^2)
2			2.5	10.1	3.2	0.7	395	36
5a	Ph	–CO–	3.0	9.9	3.2	1.0	364	48
5b	3,4-F_2-Ph	–SO_2–	2.5	10.0	3.4	1.1	436	74
5d	Benzyl	–CO–	4.9	9.9	3.3	1.1	378	48
5e	1-Naphthalene	–CO–	4.2	9.9	4.4	2.2	414	48

[a] Binding assay was performed as in Ref. 26; K_i data were presented as an average of multiple experiments ($n \geqslant 3$). Standard deviation <50%; ND = not determined.

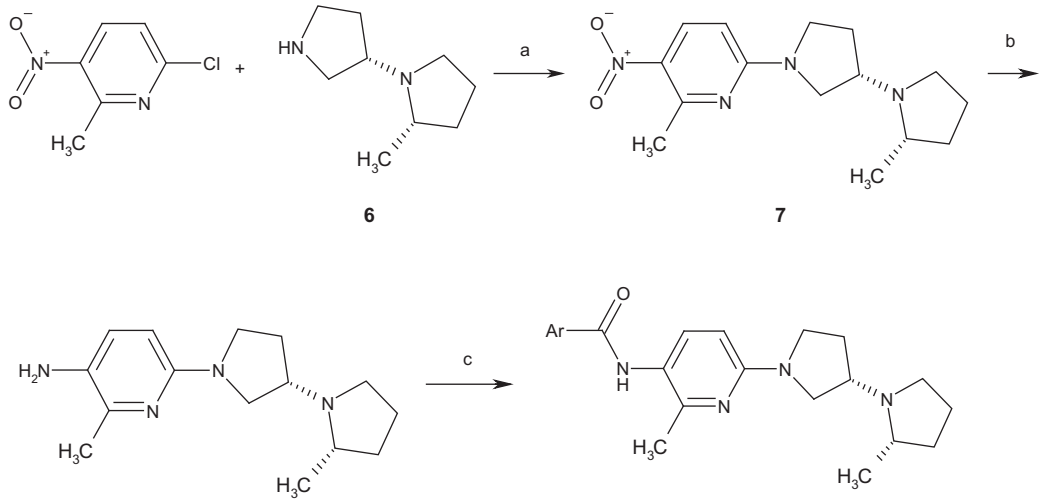

6 7

8 5

Scheme 2. Syntheses of analogs **5a**–**5e**. Reagents and conditions: (a) powdered potassium carbonate, DMSO, 85 °C (external temperature), overnight, 87% yield; (b) 5% Pd/C, MeOH, H_2 (40 psi), rt, 4 h. 100% yield; (c) ArCOCl, CH_2Cl_2, pyridine, rt, 16 h, 62% yield; or $ArCO_2H$, CH_2Cl_2, DMF, EDC, HOBt, *N*-methyl-morpholine, rt, overnight, 75–82% yield.

calculated values into a more desirable range. However, the previous SAR studies[26,27] suggested that introduction of polar groups on the terminal aromatic ring was detrimental to H_3R affinity.

Rather than taking heteroatom-containing functional groups as substituents at the terminal and the central aromatic rings to lower $c\log P$ and increase PSA, we chose hetero-aryl, the 'embedded' heteroatoms, to replace the corresponding aromatic rings. In addition, our continued optimization started from the lead (**2**) with the preferred *S*,*S* stereochemistry which was superior in H_3R affinity.[28]

Our first attempt was to investigate whether or not we could replace the terminal substituted aryl in lead (**2**) with a substituted hetero-aryl without compromising H_3R affinity while lowering $c\log P$ and increasing PSA; therefore analogs of the general type **3** were designed (Fig. 1).

Analogs **3a**–**3h** (Table 1) were synthesized according to Scheme 1 by coupling commercially available hetero-aryl acid chlorides with the chiral amine **4**[28] in DCM catalyzed by pyridine in good yield.

The analogs **3a**–**3h** were evaluated in an H_3R binding assay by displacement of [^{3}H]*N*-α-methyl-histamine in membranes isolated from a CHO cell line stably transfected with the recombinant rhesus monkey H_3 receptor (rh-H_3R)[26] (Table 1). Gratifyingly, substituted hetero-aryl replacement of aryl in **2** did not cause a substantial drop in H_3R affinity for most of the compounds. As

Table 3
In vitro profiling of **3h**

Profiling assays	Results	Conditions
hERG	IC_{50} = 37 μM	Patch-clamp technique in the whole-cell configuration on Chinese hamster ovary (CHO) cells
Ames II test	Negative	Concentrations ranged from 3 to 1000 μg/mL
MNT in vitro	Negative	Concentration ranged from 5 to 950 μg/mL in the presence or absence of metabolic activation by human liver microsomes
In silico prediction of phopholipidosis risk[34]	Low risk	
Panel screen (CEREP)	% Inhibition in binding assay <50%, except σ (1 and/or 2): 73% inhibition @ 10 μM	78 receptors, 16 enzymes, 26 kinases, and 38 ion channels
Metabolic lability in liver microsomes	<5% Metabolized	Human, mouse, rat, rabbit, macaque and dog, except in guinea pig in which 35% of **3h** was metabolized
Metabolic stability in plasma	<5% Metabolized (the compound was spiked to each of the blank plasmas at a concentration of 100 ng/ml. The spiked plasma samples were incubated in a water bath at 37 °C for up to 4 h)	Human, mouse, rat, rabbit, macaque and dog.
Intrinsic clearance in human hepatocytes	Cl = 0.040 ± 0.010 mL h^{-1} (10^6 hepatocytes)$^{-1}$ (n = 4)	
Cyp induction for CYP1A1, CYP1A2, and CYP3A4	No induction	Drug concentration ranged from 1 to 60 μM.
MBI	No inhibition	
Cyp inhibition (IC_{50}) for 3A4, 2C9, 2C19	IC_{50} >100 μM	Incubated for 4 h at 37 °C

Table 4
Pharmacokinetics of **3h** in male OF1 mice and male Sprague-Dawley rats

		Male OF1 mice[a]		Male Sprague-Dawley rats[b]	
		Plasma	Brain	Plasma	Brain
iv	$AUC_{0-\infty}$ (ng h/mL)	670	1100	1100	1200
	$t_{1/2}$ (h)	0.65	0.93	1.2	1.8
	Cl (L h/kg)	3.0		1.8	
	V_d (L/kg)	1.7		2.8	
po	$AUC_{0-\infty}$ (ng h/mL)	1900	3100	3150	3400
	C_{max} (ng/mL)	1680	2620	749	599
	t_{max} (h)	0.17	0.17	0.5	1.0
	$t_{1/2}$ (h)	1.8	4.7	7.8	9.4
	F (%)	57		56	
	B/P ratio[c]		1.6		1.1

[a] Administration at 2 mg/kg iv and 10 mg/kg *po*; iv formulation: 50% 1-methyl-2-pyrrolidinone in saline; concentration = 1.0 mg/mL, dosing 2 mL; *po* formulation: 5% DMSO/0.5% MC/0.2% Tween80, concentration = 1.0 mg/mL; dosing 10.0 mL.
[b] Administration at 2 mg/kg iv and 10 mg/kg *po*; iv formulation: saline, concentration = 0.5 mg/mL; dosing 4.0 mL; *po* formulati.on: 0.5% MC/0.2% T80; concentration = 1.0 mg/mL, dosing 10 mL.
[c] B/P ratio is brain to plasma ratio calculated with iv $AUC_{0-\infty}$ exposure.

for the 5-membered hetero-aryl derivatives **3b**–**3h**, a certain SAR trend was obvious. Particularly, the *c*log*P*, *c*log*D*, and PSA were substantially improved for all the compounds compared to lead **2**.

Next, the tolerability of replacing the central core aromatic ring by a hetero-aromatic ring was explored and analogs **5a**–**5e** (Table 2) was designed. The syntheses of analogs **5a**–**5e** (Scheme 2) commenced from the condensation of the commercially available 6-chloro-2-methyl-3-nitro-pyridine with the amine **6**[28] to yield an adduct (**7**). Hydrogenation of the nitro compound **7** afforded amine (**8**) which was coupled with aryl acid chlorides or sulfonyl chlorides to obtain the designed analogs **5a**–**5e**.

The H_3R affinity data of analogs **5a**–**5e** are listed in Table 2. Introduction of heteroatoms in the central core had little effect on H_3R affinity. Interestingly, *c*log*P* of these compounds was not substantially lowered as compared to the lead (**2**).

In consideration of the multiple parameters of H_3R affinity and physico-chemical properties in a balanced manner, **3h** excelled. The compound displayed a rh-H_3R K_i of 0.3 nM with the most noticeable improvements being a reduced *c*log*P* (3.2 → 2.8), *c*log$D_{7.4}$ (0.7 → 0.4), and an increased PSA (35.6 → 61.6) as compared to the lead (**2**) (physico-chemical properties were calculated

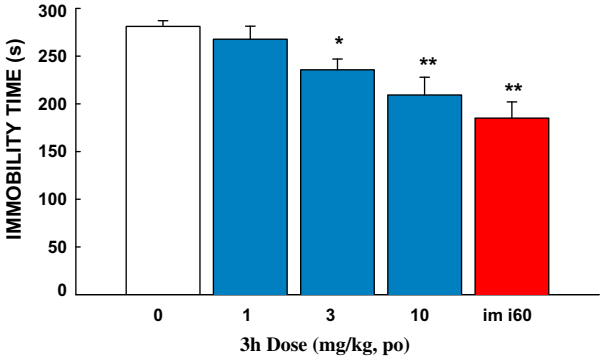

Figure 2. Forced-swimming test in rats. Dose–response relationship of **3h** (formulation: MC/0.6% + H_2O) dosing at mg/kg, *po*; Positive control: imipramine (60 mg/kg, *po*).

using ACD/Labs methods). Compound **3h** displayed an affinity for human and rat H_3R with K_i values of 0.1 and 0.9 nM, respectively. In a human H_3 (H445)-CHO-CRE-Luc assay, **3h** showed an EC_{50} of 0.7 nM (n = 1). The crystalline free base of **3h**[34] showed a good solubility (0.11 mg/mg in water, >2 mg/mL in GI track simulated media). Compound **3h** was further profiled (see Table 3). There were no significant issues identified which prohibited the development of **3h**. Particularly, **3h** showed a low risk of phospholipidosis induction potential in our internal in silico screen.[35]

When dosed at 10 mg/kg, *po*, **3h** displayed low plasma clearance and elimination half-life ($t_{1/2}$ = 1.8 h, mice; $t_{1/2}$ = 7.8 h, rat), high exposure (1900 ng h/mL, mice, 3150 ng h/mL, rat, respectively) and good oral bioavailability (57% in mice, 56% in rat) (Table 4). The brain exposures in mice and rats were 3100 ng h/mL and 3400 ng h/mL, respectively. The corresponding brain to plasma ratios were 1.6 and 1.1 for mice and rats, respectively. These results indicated a good correlation between in vivo PK and in vitro ADME data (Table 4).

The in vivo pharmacology of **3h** was then studied for anti-depression-like effects in rats. The compound dose-dependently decreased the immobility time in the forced swimming test. The reduction of immobility time was significant at 3 and 10 mg/kg with imipramine (60 mg/kg, *po*) as a positive control (Fig. 2).

The effects of **3h** on hERG current were investigated in vitro using patch-clamp technique in the whole-cell configuration on

Chinese hamster ovary (CHO) cells stably transfected with the human gene of ERG. Compound **3h** inhibited hERG current with an IC_{50} of 37 μM ($n = 4$). The effect of **3h** on canine ERG (cERG) current was investigated in vitro using patch-clamp technique in the whole-cell configuration on CHO cells stably transfected with the canine gene of ERG. **3h** inhibited cERG current with an IC_{50} of 44 μM ($n = 4$).

In the in vivo drug safety assessment, **3h** was first evaluated in group toxicity (an acute oral evaluation of behavioral side effects in mice). Compound **3h** was well tolerated and showed no evidence of any behavioral side effects (social interaction, motility, preconvulsant and convulsions) at doses of 30 mg/kg, *po*. Tremors were observed at a dose of 100 mg/kg *po* only. This result was confirmed in an independent oral exploratory general behavior study (Irwin test) in male mice. There were no behavioral, neurologic, or autonomic effects observed when **3h** was administrated orally at 0, 10, and 30 mg/kg. The MED for FST is 10 mg/kg; the tolerable dose is 30 mg/kg. Therefore, TI for mouse was estimated to be 3×.

The effects of **3h** in isolated guinea pig hearts ($n = 3$) were studied at concentrations from 0.1 to 30 μM. Compound **3h** induced a negligible effect on the coronary pressure, suggesting no effect on coronary smooth muscle cells; and a weak to moderate decrease on the ventricular contraction at higher concentrations (23% decrease at 10 μM, 33% decrease at 30 μM), indicating an inhibition of L-type calcium current.

In conclusion, lead optimization guided by histamine H_3 receptor (H_3R) affinity and calculated physico-chemical properties enabled simultaneous improvement in potency and PK properties leading to the identification of a potent, selective, devoid of hERG issues, orally bioavailable, and CNS penetrable H_3R antagonist/inverse agonist **3h**. The compound was active in forced-swimming tests suggesting its potential therapeutic utility as an anti-depressive agent. After assessment of the cardiovascular and neuropsychological/behavior safety of **3h**, the compound was extensively profiled as a pre-clinical candidate.

Acknowledgments

The authors greatly appreciate Sanofi R&D management for the strong support, H_3R project team members for their contributions, the Sanofi analytical department for their support on analytical studies in confirmation of the structures, solid state characterizations and formulation support, and the Sanofi DMPK and toxicology department for PK and in vitro/in vivo safety assessments.

References and notes

1. Arrang, J. M.; Garbarg, M.; Schwartz, J. C. *Nature* **1983**, *302*, 832.
2. Lovenberg, T. W.; Roland, B. L.; Wilson, S. J.; Jiang, X.; Pyati, J.; Huvar, A.; Jackson, M. R.; Erlander, M. G. *Mol. Pharmacol.* **1999**, *55*, 1101.
3. Yao, B. B.; Sharma, R.; Cassar, S.; Esbenshade, T. A.; Hancock, A. A. *Eur. J. Pharmacol.* **2003**, *482*, 49.
4. Hancock, A. A.; Esbenshade, T. A.; Krueger, K. M.; Yao, B. B. *Life Sci.* **2003**, *73*, 3043.
5. Pollard, H.; Moreau, J.; Arrang, J. M.; Schwartz, J. C. *Neuroscience* **1993**, *52*, 169.
6. Rouleau, A.; Heron, A.; Cochois, V.; Pillot, C.; Schwartz, J. C.; Arrang, J. M. *J. Neurochem.* **2004**, *90*, 1331.
7. Pillot, C.; Heron, A.; Schwartz, J. C.; Arrang, J. M. *Eur. J. Neurosci.* **2003**, *17*, 307.
8. Tardivel-Lacombe, J.; Rouleau, A.; Heron, A.; Morisset, S.; Pillot, C.; Cochois, V.; Schwartz, J. C.; Arrang, J. M. *NeuroReport* **2000**, *11*, 755.
9. Berlin, M.; Boyce, C. W.; Ruiz Mde, L. *J. Med. Chem.* **2011**, *54*, 26.
10. Brioni, J. D.; Esbenshade, T. A.; Garrison, T. R.; Bitner, S. R.; Cowart, M. D. *J. Pharmacol. Exp. Ther.* **2011**, *336*, 38.
11. Lin, J. S.; Sergeeva, O. A.; Haas, H. L. *J. Pharmacol. Exp. Ther.* **2011**, *336*, 17.
12. Panula, P.; Nuutinen, S. *J. Pharmacol. Exp. Ther.* **2011**, *336*, 9.
13. Passani, M. B.; Blandina, P.; Torrealba, F. *J. Pharmacol. Exp. Ther.* **2011**, *336*, 24.
14. Schwartz, J. C. *Br. J. Pharmacol.* **2011**, *163*, 713.
15. Chen, P. Y.; Tsai, C. T.; Ou, C. Y.; Hsu, W. T.; Jhuo, M. D.; Wu, C. H.; Shih, T. C.; Cheng, T. H.; Chung, J. G. *Mol. Med. Rep.* **2012**, *5*, 1043.
16. Bitner, R. S.; Markosyan, S.; Nikkel, A. L.; Brioni, J. D. *Neuropharmacology* **2011**, *60*, 460.
17. Ligneau, X.; Perrin, D.; Landais, L.; Camelin, J. C.; Calmels, T. P.; Berrebi-Bertrand, I.; Lecomte, J. M.; Parmentier, R.; Anaclet, C.; Lin, J. S.; Bertaina-Anglade, V.; la Rochelle, C. D.; d'Aniello, F.; Rouleau, A.; Gbahou, F.; Arrang, J. M.; Ganellin, C. R.; Stark, H.; Schunack, W.; Schwartz, J. C. *J. Pharmacol. Exp. Ther.* **2007**, *320*, 365.
18. Vohora, D.; Bhowmik, M. *Front. Syst. Neurosci.* **2012**, *6*, 72.
19. F Egan, M.; Zhao, X.; Gottwald, R.; Harper-Mozley, L.; Zhang, Y.; Snavely, D.; Lines, C.; Michelson, D. *Schizophr. Res.* **2013**, *146*, 224.
20. Mahmood, D.; Khanam, R.; Pillai, K. K.; Akhtar, M. *Pharmacol. Rep.* **2012**, *64*, 191.
21. Inocente, C.; Arnulf, I.; Bastuji, H.; Thibault-Stoll, A.; Raoux, A.; Reimao, R.; Lin, J. S.; Franco, P. *Clin. Neuropharmacol.* **2012**, *35*, 55.
22. Medhurst, S. J.; Collins, S. D.; Billinton, A.; Bingham, S.; Dalziel, R. G.; Brass, A.; Roberts, J. C.; Medhurst, A. D.; Chessell, I. P. *Pain* **2008**, *138*, 61.
23. Yoshimoto, R.; Miyamoto, Y.; Shimamura, K.; Ishihara, A.; Takahashi, K.; Kotani, H.; Chen, A. S.; Chen, H. Y.; Macneil, D. J.; Kanatani, A.; Tokita, S. *Proc. Natl. Acad. Sci. U.S.A.* **2006**, *103*, 13866.
24. Sander, K.; Kottke, T.; Stark, H. *Biol. Pharm. Bull.* **2008**, *31*, 2163.
25. Gemkow, M. J.; Davenport, A. J.; Harich, S.; Ellenbroek, B. A.; Cesura, A.; Hallett, D. *Drug Discovery Today* **2009**, *14*, 509.
26. Gao, Z.; Hurst, W. J.; Guillot, E.; Czechtizky, W.; Lukasczyk, U.; Nagorny, R.; Pruniaux, M. P.; Schwink, L.; Sanchez, J. A.; Stengelin, S.; Tang, L.; Winkler, I.; Hendrix, J. A.; George, P. G. *Bioorg. Med. Chem. Lett.* **2013**, *23*, 3416.
27. Gao, Z.; Hurst, W. J.; Guillot, E.; Czechtizky, W.; Lukasczyk, U.; Nagorny, R.; Pruniaux, M. P.; Schwink, L.; Sanchez, J. A.; Stengelin, S.; Tang, L.; Winkler, I.; Hendrix, J. A.; George, P. G. *Bioorg. Med. Chem. Lett.* **2013**, *23*, 3421.
28. Gao, Z.; Hurst, W. J.; Guillot, E.; Nagorny, R.; Pruniaux, M. P.; Hendrix, J. A.; George, P. G. *Bioorg. Med. Chem. Lett.* **2013**, *23*, 4044.
29. Rodriguez Sarmiento, R. M.; Nettekoven, M. H.; Taylor, S.; Plancher, J. M.; Richter, H.; Roche, O. *Bioorg. Med. Chem. Lett.* **2009**, *19*, 4495.
30. Wager, T. T.; Pettersen, B. A.; Schmidt, A. W.; Spracklin, D. K.; Mente, S.; Butler, T. W.; Howard, H.; Lettiere, D. J.; Rubitski, D. M.; Wong, D. F.; Nedza, F. M.; Nelson, F. R.; Rollema, H.; Raggon, J. W.; Aubrecht, J.; Freeman, J. K.; Marcek, J. M.; Cianfrogna, J.; Cook, K. W.; James, L. C.; Chatman, L. A.; Iredale, P. A.; Banker, M. J.; Homiski, M. L.; Munzner, J. B.; Chandrasekaran, R. Y. *J. Med. Chem.* **2011**, *54*, 7602.
31. Levoin, N.; Labeeuw, O.; Calmels, T.; Poupardin-Olivier, O.; Berrebi-Bertrand, I.; Lecomte, J. M.; Schwartz, J. C.; Capet, M. *Bioorg. Med. Chem. Lett.* **2011**, *21*, 5378.
32. Ploemen, J. P.; Kelder, J.; Hafmans, T.; van de Sandt, H.; van Burgsteden, J. A.; Saleminki, P. J.; van Esch, E. *Exp. Toxicol. Pathol.* **2004**, *55*, 347.
33. Pelletier, D. J.; Gehlhaar, D.; Tilloy-Ellul, A.; Johnson, T. O.; Greene, N. *J. Chem. Inf. Model.* **2007**, *47*, 1196.
34. *Analytical of **3h**:* LCMS: LC method: SYNERGI 2U HYDRO-RP 20 × 4.0 mm column, 0.1% TFA in water/acetonitrile 5–40% acetonitrile in 2 min then, to 95% acetonitrile at 5 min at flow rate of 1.0 mL/min; LCMS: $t_R = 1.54$ min, MS: 383 ($M+H^+$).
^{1}H NMR ($CDCl_3$, 300 MHz), δ (ppm): 7.44 (m, 1H), 6.92 (br s, 1H), 6.40 (br s, 1H), 6.39 (bs, 1H), 3.50 (m, 1H), 3.4–3.2 (m, 4H), 3.00 (m, 1H), 2.78 (m, 1H), 2.66 (br s, 3H), 2.48 (br s, 3H), 2.5 (m, 1H), 2.26 (s, 3H), 2.18 (m, 1H), 2.00 (m, 2H), 1.79 (m, 2H), 1.48 (m, 1H), 1.14 (d, 6.3 Hz, 3H). Calcd for $C_{22}H_{30}N_4O_2$ 382.4992; C 69.08, H 7.91, N 14.65, O 8.37; Found: C 69.05, H 8.17, N 14.69; Optical rotation: $[\alpha]_D$ +27.45° (*c* 0.532, MeOH); Chiral purity: 100% (chiral HPLC).
35. Proprietary internal in silico model prediction. The model is based on carefully filtered internal experimental data. It was developed using relevant two-and three dimensional descriptors to capture molecular properties like shape, lipophilicity and electrostatic potential combined with powerful statistical methods. The model was carefully validated using test sets of novel molecules.